Los Alamos Environmental Restoration Records Management Facility

ER Record I.D.# 59118

LOS ALAMOS NATIONAL LABORATORY
ENVIRONMENTAL RESTORATION
Records Processing Facility
ER Records Index Form

ER ID NO. 59118 *Date Received:* 9/4/98 *Processor:* YCA *Page Count:* 19

Privileged: (Y/N) N *Record Category:* P *Record Package No:* 0

FileFolder: N/A

Correction: (Y/N) N *Corrected No.* 0 *Corrected By Number:* 0

Administrative Record: (Y/N) Y

Refilmed: (Y/N) N *Old ER ID Number:* 0 *New ER ID Number:* 0

Miscellaneous Comments:
REFERENCE CITED

14235

THIS FORM IS SUBJECT TO CHANGE. CONTACT THE RPF FOR LATEST VERSION. (JUNE 1997)

(19)

LA-UR-96-4682

59118

Vadose Zone Water Movement at Area G , Los Alamos National Laboratory, TA-54: Interpretations Based on Chloride and Stable Isotope Profiles

Brent D. Newman

Environmental Science Group, EES-15

Los Alamos National Laboratory

December 9, 1996

Received by ER-RPF

SEP 0 4 1998

MA

ABSTRACT

Natural chloride and stable isotope tracers were used to examine the vadose zone hydrology of Mesita del Buey in the vicinity of the Los Alamos National Laboratory, Area G, Low-Level Radioactive Waste Facility. Pore-water chloride concentrations were measured with depth from core samples from four wells. In addition, $\delta^{18}O$ and δD stable isotope profiles were determined for one of the wells. The objectives of the study were to (1) quantify flux rates and pore water ages using the chloride data; (2) compare water flux rates to those obtained from hydraulic methods in order to estimate the most appropriate values for use in performance assessment modeling; and (3) examine stable isotope profiles for evidence of deep evaporation in the mesa system. In general, the chloride results indicate flux rates of a few mm/yr in the upper and lower parts of the mesa. All the wells have a zone of high chloride concentration at approximately mid-depth. Fluxes in these chloride bulge areas range from 0.03 to 0.8 mm/yr. It is likely that the bulges and low flux values may be related to evaporative removal of water in the mesa. However, differences in maximum chloride concentrations (e.g., 232 mg/L in well 1107 vs. 4755 mg/L in well 1117) suggest that there may be substantial lateral variability in the amount of evaporation that occurs. The chloride-based fluxes are reasonably consistent with those from hydraulic approaches. The chloride results also suggest that there is substantial lateral and vertical variability in the mesa hydrologic system. Finally, the stable isotope results indicate the

presence of isotopically heavy water in the same region as the chloride bulge. Isotopically heavy water indicates that deep evaporation is likely because the largest values occur at depths much greater than the depths at which solar-driven surface evaporation takes place.

INTRODUCTION

Evaluating representative flux rates for the Mesita del Buey vadose zone is crucial for performance assessment of the Area G Low-Level Radioactive Waste Facility located at the LANL TA-54. The hydraulic approach (e.g., Birdsell et al., 1995; Rogers and Gallaher, 1995) is one way that vadose zone fluxes can be estimated. However, because of the difficulty in measuring hydraulic properties and accurately determining moisture content, suction, and hydraulic conductivity relationships, the hydraulic approach yields flux estimates with large uncertainties. Thus, even though the hydraulic approach provides useful information, additional estimates of the flux that do not rely on the same assumptions or parameters as the hydraulic approach is beneficial. The additional estimates would provide increased confidence that representative flux values are used in the performance assessment process. The current study was designed to provide estimates of flux based on the chloride mass balance method (Allison et al., 1994; Stone, 1984). Because this is a tracer-based, and not a hydraulic-based approach, it provides the independent estimates of flux that are needed.

In addition to flux estimates, conceptual models of mesa hydrology can be refined using natural tracer studies.] In particular, stable isotopes can be used to evaluate evaporation, both at the mesa surface and at depth. The isotopic composition of water is affected by evaporation, which preferentially extracts light isotopes into the vapor phase, leaving the remaining liquid enriched in heavy isotopes. The depth at which δD and $\delta^{18}O$ reach their maximum (heaviest) values coincides with the depth of evaporation (Barnes and Allison, 1983; Allison et al., 1983). Deep evaporation in Mesita del Buey, in contrast to surface evaporation, has been suggested by Rogers and Gallaher (1995); Rogers et al. (1996); and Vold et al. (1997) based on data from moisture content and matric potential measurements. The idea of evaporative removal of water from mid-mesa depths of approximately 15 to 100 ft is untested, and will significantly influence contaminant mobility affecting performance assessment calculations.

Based on the need for independent estimates of flux and for testing the deep evaporation hypothesis, the objectives of this study were to (1) use natural chloride tracers to estimate flux rates of water in mesas and the age of water in the vadose zone water; (2) compare the chloride-based fluxes to hydraulic-based fluxes currently used to model vadose zone behavior at Area G; and (3) examine stable isotope data for evidence of deep evaporative removal of water within the mesa.

MATERIALS AND METHODS

Chloride Sampling and Laboratory Analyses

Chloride profiles were determined from core samples from wells 54-1107, 54-1117, 54-1121, and 54-1123 at Area G. Samples were collected and analyzed at 5- or 10-ft intervals. Chloride concentrations were determined by leaching the core samples with DI water and analyzing the leachate using ion chromatography. The leaching and analyses were performed at the Los Alamos EES-1 geochemistry laboratory. For each sample, approximately 50 g of tuff was crushed using a mortar and pestle. The tuff was then oven dried for at least 12 hours at 100°C. The dry sample was weighed and added to an Erlenmeyer flask along with approximately 75 g of DI water. The flask was agitated for 24 hours on a rotary mixer. Once the mixer was turned off and the solid material settled, the supernatant was filtered and analyzed using a Dionex Ion Chromatograph. Analytical precision of the ion chromatograph is better than 5 %.

Pore water chloride concentrations were calculated using the leachate concentrations, volumetric moisture contents (from Vold, 1996), and bulk densities (from Krier et al., 1995) for each well (see Appendix 1). The pore water chloride concentrations were then used in the chloride mass balance approach described below to estimate vertical fluxes and vadose water ages.

Chloride Mass Balance Approach

The chloride mass balance approach has been successfully used to determine vadose zone fluxes in semiarid and arid locations worldwide. The approach involves measuring chloride concentrations in vadose zone water with depth. These concentrations serve as indicators of downward flux and water age (Stone, 1984; Allison et al., 1994). The downward flux is inversely proportional to the amount of chloride accumulation: high chloride concentrations indicate a low flux that represents many years of meteoric chloride accumulation coupled with evapotranspirative removal of water. Relatively low chloride contents indicate a high downward flux, or water that is able to move through the vadose zone at a fast enough rate to minimize evapotranspiration effects.

The chloride mass balance method is based on the following assumptions: 1) flow occurs largely as downward piston flow; 2) dispersive mixing of water and chloride is small; 3) atmospheric chloride deposition has been relatively constant and is the sole source of chloride to the system; and 4) chloride uptake by plants is negligible. Uncertainty related to these assumptions will be addressed in the Discussion section.

If vadose zone chloride concentrations are constant below the root zone, then the average annual flux (or recharge rate) can be estimated using

$$R = P \cdot Cl_p / C_{sw}, \quad (1)$$

were R is the flux (m/yr); P is the average annual precipitation rate (m/yr); Cl_p is the average concentration of chloride in bulk precipitation (g/m^3); and C_{sw} is the chloride concentration in vadose-zone water below the root zone (g/m^3). However, chloride concentrations in deep profiles are sometimes not constant below the root zone. In this case, plots of cumulative chloride as a function of cumulative water in the profile can be used to determine changes in recharge rates over time. Approximately linear segments on the cumulative-cumulative plots indicate zones of constant flux. The flux for a segment is given by

$$R = (Cl_p \cdot P) / Cl_{seg}, \quad (2)$$

where Cl_{seg} is the average chloride content of the samples represented by the segment (g/m^3). Chloride-based vadose water ages can also be estimated by first calculating the amount of chloride in each sample interval down to the depth of interest using the relationship

$$Cl_i = \theta \cdot C_{cl} \cdot Z \quad (3)$$

where Cl_i is the amount of chloride in the interval (g/m^2), θ is the volumetric moisture content in the interval, C_{cl} is the mass of chloride in the interval per volume of rock (g/m^3), and Z is the length of the sample interval (m). By calculating the cumulative sum of the Cl_i values down to the depth of interest, the age can be calculated using

$$A = Cl_{cum}/(Cl_p \cdot P), \quad (4)$$

where A is age in years, and Cl_{cum} is the cumulative sum of the Cl_i values (g/m^2) at a given depth. A value of 0.36 m/yr was used for the average annual precipitation (P) based on measurements at TA-54 (Bowen, 1990), and a value of 0.29 g/m^3 was used for the average concentration of chloride in bulk precipitation (Cl_p) based on Anderholm (1994).

Stable Isotope Analyses

Stable isotope analyses of pore waters from Area G were conducted using moisture-protected samples from well 54-1117. The moisture-protected system involves sealing core samples in gas impermeable plastic bags as the cores were removed from the core barrel during drilling. This procedure reduces the chance of pore water evaporation during the period between sampling and analysis which would alter the isotopic composition of the water.

The stable-isotope analyses were carried out at the New Mexico Tech Stable Isotope Laboratory. Soil water was extracted by high-temperature vacuum distillation, following Shurbaji et al. (1995), and $\delta^{18}O$ and δD measurements were made on a Finnegan-Mat, Delta-E stable-isotope-ratio mass spectrometer using OZ-Tech gas standards. The hydrogen and oxygen isotopes are reported in delta (δ) notation as per mil (‰) differences relative to the V-SMOW international standard:

$$\delta D \text{ or } \delta^{18}O = \left[\frac{R_{sample} - R_{SMOW}}{R_{SMOW}}\right] \times 1000, \qquad (5)$$

where R is the D/H or $^{18}O/^{16}O$ ratio. The value of $\delta^{18}O$ was measured from extractions made using the carbon dioxide equilibration technique of Socki et al. (1992). For the δD analyses, hydrogen was extracted using the hot uranium method of Bigeleisen et al. (1952), and the analyses were corrected by means of a linear equation ($\delta D_{actual} = 1.008\delta D_{measured} + 7.378$) based on regression analysis of V-SMOW and GISP standards. The analytical precision for the $\delta^{18}O$ and δD analyses by mass spectroscopy is better than ±0.2 ‰ and ±6 ‰, respectively. Two of the distillates (the 16.6 and 25.6 ft samples) did not yield reasonable δD values. It is likely that some hydrogen was produced from organic material, possibly from decayed roots, invalidating the water δD values.

RESULTS

Chloride profiles for the four wells are shown in Figure 1. The chloride concentrations are not constant with depth, and each profile shows a distinct bulge of high concentration between the 15 to 80 ft depths. The changes in chloride concentrations generally correspond to changes in volumetric moisture content where the chloride bulges occur in the zone of low moisture content (Figure 2).

Because the chloride concentrations were not constant with depth, the cumulative chloride-cumulative water approach was used to calculate fluxes (values used in the flux and age calculations are given in Appendix 1). Cumulative-cumulative plots for each well are shown in Figure 3. The figures show three approximately linear segments, with well 1107 having a possible fourth segment below the vapor phase notch. Flux rates were calculated for the three segments for each well (Table 1). For the upper segments that correspond to the shallowest depths, relatively high flux rates are indicated as compared to the middle segment. Wells 1107 and 1121 yield flux rates of 6 and 3 mm/yr, respectively, whereas the upper segments for wells 1117 and 1123 yield rates of 0.1 and 1.5 mm/yr. The reason that the 1117 and 1123 rates are so much lower than those of 1107 and 1121 is that shallow samples were not available for 1117 and 1123 and these would tend to have lower chloride concentrations which would increase the flux estimates. Flux rates are the lowest in each of the wells for the middle segments and range from 0.03 to 0.8 mm/yr. For the deepest segments, the flux rates increase to values similar to that of the upper segments. Again, there were no samples available deeper than about 90 ft for wells 1117 and 1123 and thus, the estimates of deep flux rates are substantially lower than those from 1107 and 1121 because only a few low chloride concentration samples were available.

Chloride accumulation ages for each well are also shown in Table 1. Ages for well 1107 suggest that it takes between one to two thousand years to

reach the 125 ft depth. Ages for the other wells suggest that it takes approximately six thousand years or more to reach the same depth.

The stable isotope profiles for well 1117 are shown in Figure 4. The trend is for the pore waters to become lighter in both $\delta^{18}O$ and δD with depth. Because there were no moisture-protected samples available for depths less than 16 ft, generalized curves for shallow isotope profiles at TA-51 (Newman et al., 1996) are also shown in Figure 4. TA-51 is on the same mesa as Area G, approximately 3 km upslope, and is probably a good proxy for undisturbed conditions at Area G. The TA-51 curves show that solar-induced surface evaporation is limited to shallow depths. By a depth of 1-2 meters, isotopic values become lighter (-9 to -10 $\delta^{18}O$ and -80 to -95 δD). At the depth that the well 1117 data start, isotopic values are substantially heavier than the 1-2 meter samples from TA-51. This difference is important for evaluating deep evaporative processes and will be explained further below.

DISCUSSION

Significance of the Chloride Bulges

The chloride bulges (Figure 1) are important features of the vertical profiles because the origin of these chloride accumulations will affect the development of conceptual and quantitative models of the mesa hydrologic system. One explanation is that the bulges represent a past period of low percolation rates and high evapotranspiration which was followed by a period

of higher percolation rates and lower evapotranspiration that displaced the chloride bulges to the ≈20-80 ft depth. However, the vadose water ages for the bulges are not concordant. If changing paleoclimate was the cause of the chloride bulges, roughly similar peak concentrations and ages would be expected. A further problem is that the climate for the last 20000 years, though variable, has tended to be wetter than the present (Phillips et al., 1986; Stute et al., 1992). This is in direct contrast to the interpretation that the bulges indicate drier past conditions. The most likely explanation is that the bulges represent a zone of evaporation and vapor phase transport which would cause chloride to accumulate. The possible pathways of vapor movement are discussed in the Deep Evaporation section below. Evaporation seems to be a plausible explanation given that other studies have suggested the possible presence of deep zones of vapor dominated transport (e.g., Rogers and Gallaher, 1995; Rogers et al., 1996; Vold et al. 1997). The evaporative zone, if present, may not always act as a barrier to flow as indicated by the profile and flux rates for well 1107 (Figure 1, Table 1). Even though there is a chloride bulge in well 1107, the mass accumulated is a fraction of that in the other wells and the estimated vertical flux is still fairly large (0.8 mm/yr). The differences in chloride accumulation between the wells suggests that if evaporation occurs, there may be substantial lateral heterogeneity where the evaporative flux is not uniform throughout the mesa. The changes in chloride concentration appear to be correlated to certain stratigraphic units and

features. The bulge in well 1107 occurs mainly within the lower part of unit 2b (surge beds), while the bulges in wells 1117, 1121 and 1123 occur within the stratigraphically lower units, 2a and 1b. These units may act as permeable zones that have a direct connection to the atmosphere. For example, the surge beds at the base of unit 2b have been suggested as a potential evaporative zone (Rogers and Gallaher, 1995; Rogers et al., 1996) which is consistent with the chloride bulge in well 1107. The bulges in wells 1117, 1121, and 1123 overlap the surge beds in some cases, but also the lithologic contacts between units 1v(c), 1v(u1), and 1v(u2) (following the suggested nomenclature of Broxton and Reneau, 1995). These units are fractured and contain pumice beds, either of which may have a connection to the atmosphere permitting deep evaporation.

The vapor-phase notch (Figure 3) is another stratigraphic feature that appears to control or at least correlate with changes in chloride concentrations and flux rates. Chloride concentrations at and below the vapor-phase notch are dilute and the decrease in concentration corresponds to a substantial increase in moisture content at the vapor phase notch. In wells 1121 and 1123 a large change in slope occurs between the middle segment and the deepest segment of the cumulative-cumulative plots (Figures 3c and 3d), that corresponds to the vapor-phase notch. The influence of the vapor phase notch in well 1107 is more subtle (Figure 3a). The cumulative-cumulative plot for well 1107 shows a small change in slope in the deepest segment close to the vapor phase notch. If there were samples deeper in the profile, a fourth

segment below the vapor phase notch might be more readily apparent. Only one sample from below the vapor phase notch was available for well 1117, so no assessment of its influence can be made for this well.

Uncertainty

With the various assumptions used in the chloride mass balance method there are some related uncertainties. The first uncertainty relates to the 1-D vertical flow assumption. If deep evaporative processes occur, then potentially large but unquantifiable errors in the flux estimates result. From a qualitative point of view, however, a large chloride concentration associated with an evaporative zone is consistent with a low flux. Lateral flow also violates the 1-D vertical flow assumption. If there is lateral flow in the deeper units at the base of the mesa (described in the Stable Isotope section, below) then the flux estimates are suspect because lateral flow can add or remove chloride from the system. Fracture flow is not considered in the chloride mass balance approach either and because of its possible importance, especially in the shallower tuff units, fracture flow adds additional uncertainty to the flux and age estimates. Another factor that contributes to uncertainty is the concentration of chloride entering the mesa. Unfortunately, there are no long term data available for the Los Alamos area, but short term data can be used to bound the problem. A value of 0.29 g/m^3 was used in the flux and age calculations based on a chloride mass balance study by Anderholm (1994) for the Sante Fe area. This

value may be higher than the Pajarito Plateau average value, and is probably a conservative value in that it may overestimate flux rates and underestimate the ages. Evaluation of chloride concentrations in precipitation from the National Atmospheric Deposition Program station at Bandelier National Monument (NADP, 1994) and various sampling stations on the Pajarito Plateau monitored by Adams et al. (1995) suggest that chloride concentrations in rainfall might be as low as 0.1 g/m^3. If this value is more representative of the Pajarito Plateau, then the fluxes in Table 1 would be about one third less than those shown and the ages would be about three times greater. The different chloride input values do not make order of magnitude changes in the flux rates, and thus do not result in much additional uncertainty, especially when compared to uncertainties from other factors such as deep evaporation. The effects of different chloride concentrations are important considerations for correlating ages and changes in flux with past periods of climate change because some paleoclimate changes have occurred over relatively short time periods.

Comparison of Chloride-Based Flux Estimates to Other Flux Estimates

Birdsell et al. (1995) used a modeling approach to estimate flux values in the vadose zone beneath Area G. They used generalized hydraulic parameters for the different stratigraphic units and varied the infiltration rate in order to match existing in-situ saturation data. They found that the saturation profile could not be simulated using a single flux value. Instead, they used three

different flux values to match three saturation zones in the profile. Their result is consistent with the chloride results in that three main flux zones were also identified. Unfortunately, the magnitudes of the chloride-based flux rates do not agree with the simulations in some cases. For example, Birdsell et al. found that a low flux of 0 to 0.1 mm/yr fit the saturation data from unit 2b best. For the same unit, the chloride-based flux rates are 3-6 mm/yr. This discrepancy results from differences in moisture contents used in the simulations versus those used in the chloride method. The moisture contents used by Birdsell et al. were based on values for the lower part of the unit where values range from 1 to 4% volumetric. The upper part of the unit is much wetter with moisture contents on the order of 7 to 14% and these values were used in the chloride-based estimates.

There was some consistency between the simulations and the chloride results for unit 2a, in that both studies indicate unit 2a is a zone of low flux. Again, however, the chloride method yields higher flux rates than the simulations, probably because of higher moisture contents than those used in the simulations. For units 1a and 1b, the chloride-based flux rates agree with the range of flux rates from the simulations. For the Cerro Toledo and Otowi units, the chloride-based estimate for well 1121 is consistent with the simulations. Wells 1107 and 1117 were not drilled into the Cerro Toledo and Otowi units, and only one sample was available from well 1123, so no comparisons can be made for these wells.

Another comparison can be made using the flux estimates for the upper part of unit 2b. Newman et al. (1996) estimated chloride-based flux rates through various soil profiles and into the first 10-50 cm of unit 2b for an undisturbed site at TA-51. For soils without clay-rich Bt horizons, which is representative of conditions at Area G, flux rates ranged from 0.5 to 10 mm/yr. Though these estimates are dominated by soil hydraulic properties, the majority of the estimates are consistent with the 3-6 mm/yr estimates for the upper part of unit 2b at Area G. Newman et al. also noted substantial lateral variability in flux rates, consistent with the results from this study.

A final comparison can be made with the results of Vold et al. (1997) who calculated the magnitude of liquid and vapor fluxes in the mesa. Overall, the Vold et al. results are in reasonable agreement with the chloride-based flux estimates. Vapor-flux rates dominate in the middle of the mesa, which corresponds to the zone of low chloride-based flux rates, and supports the hypothesis of deep evaporation. Liquid flux rates are dominant in the region near and below the vapor phase notch, which is consistent with the increase in chloride-based flux rates in the deeper parts of the mesa.

Stable Isotopes

Stable isotope data from well 1117 (Figure 4) provide additional evidence for deep evaporation. The TA-51 data show that surface evaporation effects disappear at depths less than 6 ft whereupon values reach relatively light $\delta^{18}O$

and δD values of -9 to -10 ‰ and -80 to -95 ‰, respectively. Unsaturated zone stable isotope theory predicts that a quasi-steady state value should be reached below the zone influenced by solar surface evaporation (Allison et al., 1983; Barnes and Allison, 1983). In other words, the approximately -9 ‰ $\delta^{18}O$ value, for example, should be maintained throughout the profile for all depths below about 6 ft. However, contrary to theory, the 1117 data show quite heavy values at depths below the zone influenced by surface evaporation.

A paleoclimate interpretation for the existence of isotopically heavy values deep in the profile does not seem plausible, as explained in the chloride bulge discussion. Instead, the isotope data are consistent with evaporative removal of water from within the mesa. At present, it is not clear how this process works or what the pathways for airflow and water removal might be. One hypothesis is that dry air travels down vertical fractures in the tuff, evaporates the water and moves back out of the fractures in response to thermal or barometric changes. Alternatively, the sides of the mesa could play a role in allowing dry air into the system and moving water vapor out. The Bandelier tuff is exposed on the mesa sides and is subject to a wide range of temperatures and barometric pressures. At this stage, the tracers and low moisture contents strongly indicate that deep evaporation occurs in the mesa. However, additional isotope data are needed to confirm the behavior seen in well 1117 and more work will be required to understand the mechanisms and pathways by which the evaporation occurs.

The existence of light isotope values at the vapor phase notch at the 85 ft depth in well 1117 leads to two explanations. The first is that water infiltrated during a higher precipitation period during the Pleistocene or early to mid Holocene, and was not subject to extensive evaporation. Studies by Phillips et al. (1986) and Stute et al. (1992) indicate that such periods occurred in the past 20,000 years, so this explanation appears to be reasonable for the light water at the bottom of the profile. The second explanation is that water may have been introduced by lateral flow along pathways that were not subject to evaporation of the same intensity that occurred in the middle of the mesa. It is possible that recharge in the adjacent canyons flows underneath Mesita del Buey, and Pajarito Canyon in particular contains saturated alluvial zones which could generate lateral flow. Unfortunately, we do not have enough information about the link between mesa and canyon hydrology to adequately evaluate if lateral flow really occurs. The stable isotope data however, can provide valuable clues regarding the validity of the lateral flow hypothesis. A meteoric water plot (Figure 5) shows a well-defined evaporation trend line extending from the local meteoric water line to the right. $\delta^{18}O$ and δD values of precipitation from the Pajarito Plateau plot along the local meteoric water line, and if evaporation occurs the isotopic values will become progressively heavier following a trend such as that shown for well 1117. The evaporative trend line suggests that all of the waters in the 1117 profile have the same source, including the light water at the vapor phase notch. Thus, if lateral flow occurs,

it would have to have the same original isotopic composition as the water that was evaporated from the middle of the mesa. In other words, the source of the lateral flow would need to plot on the same evaporation trend line as the 1117 waters. Measurements of the isotopic composition of potential lateral flow sources, such as the alluvial groundwater from Pajarito Canyon, would greatly aid in resolving this question.

SUMMARY AND CONCLUSIONS

Chloride flux estimates for wells 1107, 1117, 1121, and 1123 showed reasonable similarity in overall behavior where flux rates were highest in the shallow and deeper parts of Mesita del Buey and lowest in the middle of the mesa. Flux estimates for the shallow and deep zones are on the order of a few mm/yr. For the middle region of the mesa, flux estimates ranged from 0.03 mm/yr for well 1123 to 0.8 mm/yr for well 1107. The low mid-depth fluxes in the wells are related to large concentrations of chloride. It appears that these concentrations are related to deep evaporative processes, and a stable isotope profile from well 1117 supports this conclusion. One detail is that the bulge in well 1117 has a very high maximum chloride concentration (4755 mg/L), while the bulge for well 1107 has a much lower concentration (232 mg/L). The large differences in chloride concentrations suggest that there is substantial lateral variability in vertical flux and in the amount of evaporation that occurs. In summary, it appears that the Mesita del Buey vadose zone is characterized by

substantial lateral and vertical heterogeneities that control the rates of water movement in the mesa. In addition, water movement in the middle of the mesa is likely influenced by deep evaporation. Future work will involve measuring additional isotope profiles to verify the behavior seen in well 1117, and will also include analyses of shallow isotope data from Area G so that site specific values can be used instead of those from TA-51.

ACKNOWLEDGMENTS

The author gratefully appreciates the interest and support of Diana Hollis and Erik Vold. Thanks are given to Dale Counce for performing the leachings and chloride analyses, and to Andrew Campbell, Jeff Klein, and Christa Vindum for their work on the stable isotope analyses.

REFERENCES

Adams, A. I., F. Goff and D. Counce. 1995. Chemical and Isotopic Variations of Precipitation in the Los Alamos Region, New Mexico. Los Alamos National Laboratory Report, LA-12895-MS. 35 pp.

Allison, G. B., Barnes, C. J. and Hughes, M. W. 1983. The Distribution of Deuterium and ^{18}O in Dry Soils 2: Experimental. J. Hydrol. 64: 377-397.

Allison, G. B., G. W. Gee, and S. W. Tyler. 1994. Vadose-Zone Techniques for Estimating Groundwater Recharge in Arid and Semiarid Regions. Soil Sci. Soc. of Am. J. V. 58. pp. 6-14

Anderholm, S. K. 1994. Ground-water recharge near Sante Fe, north-central New Mexico. USGS Water-Res. Invest. Rep. 94-4078. 68 pp.

Barnes, C. J., and Allison, G. B., 1983. The Distribution of Deuterium and "O in Dry Soils. 1. Theory. J. Hydrol., 60: 141-156.

Bigeleisen, J., M. L. Perlman, H. C. Prosser. 1952. Conversion of Hydrogenic Materials to Hydrogen for Isotopic Analysis. Anal. Chem., V. 24. pp. 1356-1357.

Birdsell, K. H., W. E. Soll, N. D. Rosenberg, and B. A. Robinson. 1995. Numerical Modeling of Unsaturated Groundwater Flow and Radionuclide Transport at MDA G. . Los Alamos National Laboratory Report, LA-UR-95-2735. 49 pp.

Bowen, B. M. 1990. Los Alamos Climatology. Los Alamos National Laboratory Report LA-11735-MS. 254 pp.

Broxton, D. E. and S. L. Reneau. 1995. Stratigraphic Nomenclature of the Bandelier Tuff for the Environmental Restoration Project at Los Alamos National Laboratory. Los Alamos National Laboratory Report, LA-13010-MS. 21 pp.

Krier, D., P. Longmire, R. Gilkeson, and J. Turin. 1995. Geologic, Geohydrologic, and Geochemical Data Summary of MDA G, TA-54, Los Alamos National Laboratory, Los Alamos, New Mexico. in Performance Assessment of LANL, TA-54, Area G, Low-Level Radioactive Waste Disposal Facility (DRAFT). D. Hollis, E. Vold, K. Birdsell, J. Turin, P. Longmire, E. Springer, W. Hansen, D. Krier, and R. Shuman.

National Atmospheric Deposition Program (NADP). 1994. National Trends Network NADP/NTN (NRSP-3) Site Report, Precipitation and Chemistry Data. Natural Resource Ecology Laboratory, Colorado State, Ft. Collins, CO.

Newman, B. D., A. R. Campbell, and B. P. Wilcox. 1996. Tracer-based Studies of Soil Water Movement in Semi-Arid Forests of New Mexico. Accepted for Publication in the Journal of Hydrology

Phillips, F. M., L. A. Peters, M. K. Tansey, and S. N. Davis. 1986. Paleoclimatic Inferences from an Isotopic Investigation of Groundwater in the Central San Juan Basin, New Mexico. Quat. Res. V. 26. pp. 179-193.

Rogers, D. B, and B. M. Gallaher. 1995. The Unsaturated Hydraulic Characteristics of the Bandelier Tuff. Los Alamos National Laboratory Report, LA-12968-MS.

Rogers, D. B., B. M. Gallaher, and E. L. Vold. 1996. Vadose Zone Infiltration Beneath the Pajarito Plateau at Los Alamos National Laboratory. New Mexico Geological Society 1996 Guidebook, Geology of the Los Alamos-Jemez Mountains Region. In Press.

Shurbaji, A.-R.M., Phillips, F. M., Campbell, A. R. and Knowlton, R. G. 1995. Application of a Numerical Model for Simulating Water Flow, Isotope Transport, and Heat Transfer in the Unsaturated Zone. J. Hydrol. 171: 143-163.

Socki, R. A., Karlsson, H. R. and Gibson, E. K. 1992. Extraction Technique for the Determination of Oxygen-18 in Water Using Preevacuated Glass Vials. Anal. Chem., 64: 829-831.

Stone, W. J. 1984. Recharge in the Salt Lake Coal Field Based on Chloride in the Unsaturated Zone. New Mexico Bureau of Mines and Mineral Resources, Open-File Report 214. 64 pp.

Stute, M., P. Schlosser, J. F. Clark, and W. S. Broecker. 1992. Paleotemperatures in the Southwestern United States Derived from Noble Gases in Ground Water. Science, V. 256. pp. 1000-1002.

Vold, E. 1996. Unpublished Data. Los Alamos National Laboratory.

Vold, E., B. Newman, K. Birdsell, B. Gallaher, D. Krier, P. Longmire, D. Rogers, and E. Springer. 1997. Representative Recharge Rates in a Complex Unsaturated Hydrogeology. Waste Management 97. In preparation.

Vuataz, F.-D. and Goff, F. 1986. Isotope Geochemistry of Thermal and Nonthermal Waters in the Valles Caldera, Jemez Mountains, Northern New Mexico. J. Geophys. Res., 91(B2): 1835-1853.

Table 1. Flux Estimates and Soil Water Ages for Wells 1107 and 1121, Area G

Well 1107		
Depth interval (ft)	Flux (mm/yr)	Age at bottom of depth interval (yr)
0-31	6	120
31-58	0.8	1169
66-125	5	1345

Well 1117		
Depth interval (ft)	Flux (mm/yr)	Age at bottom of depth interval (yr)
15-30	0.1	482
35-60	0.03	8295
70-85	0.2	9674

Well 1121		
Depth interval (ft)	Flux (mm/yr)	Age at bottom of depth interval (yr)
0-42	3	323
42-84	0.06	17659
89-146	5	17862

Well 1123		
Depth interval (ft)	Flux (mm/yr)	Age at bottom of depth interval (yr)
9-20.3	1.5	118
25-62.5	0.1	5507
65-90.8	0.9	5852

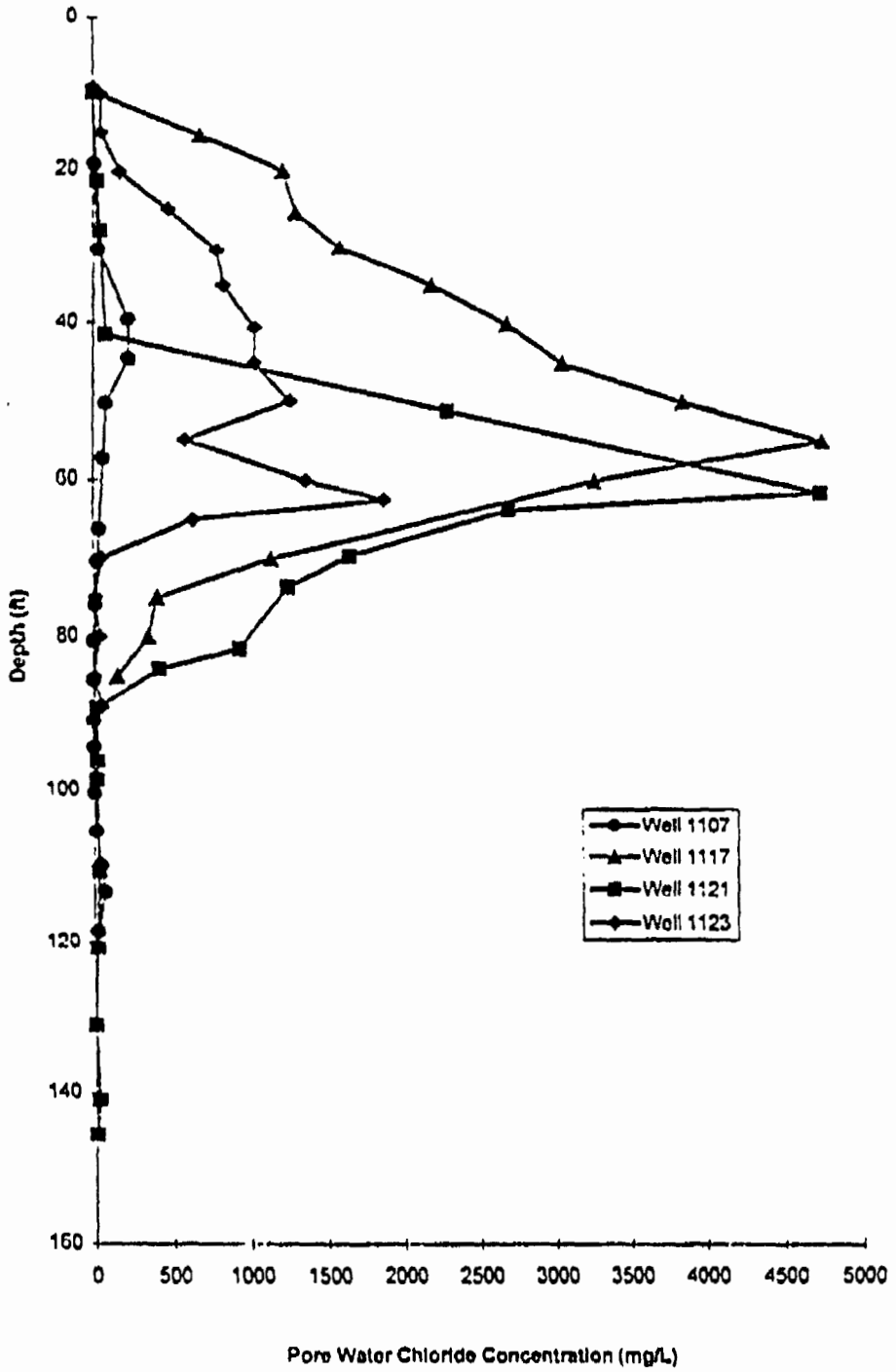

Figure 1. Chloride profiles for wells 1107, 1117, 1121, and 1123.

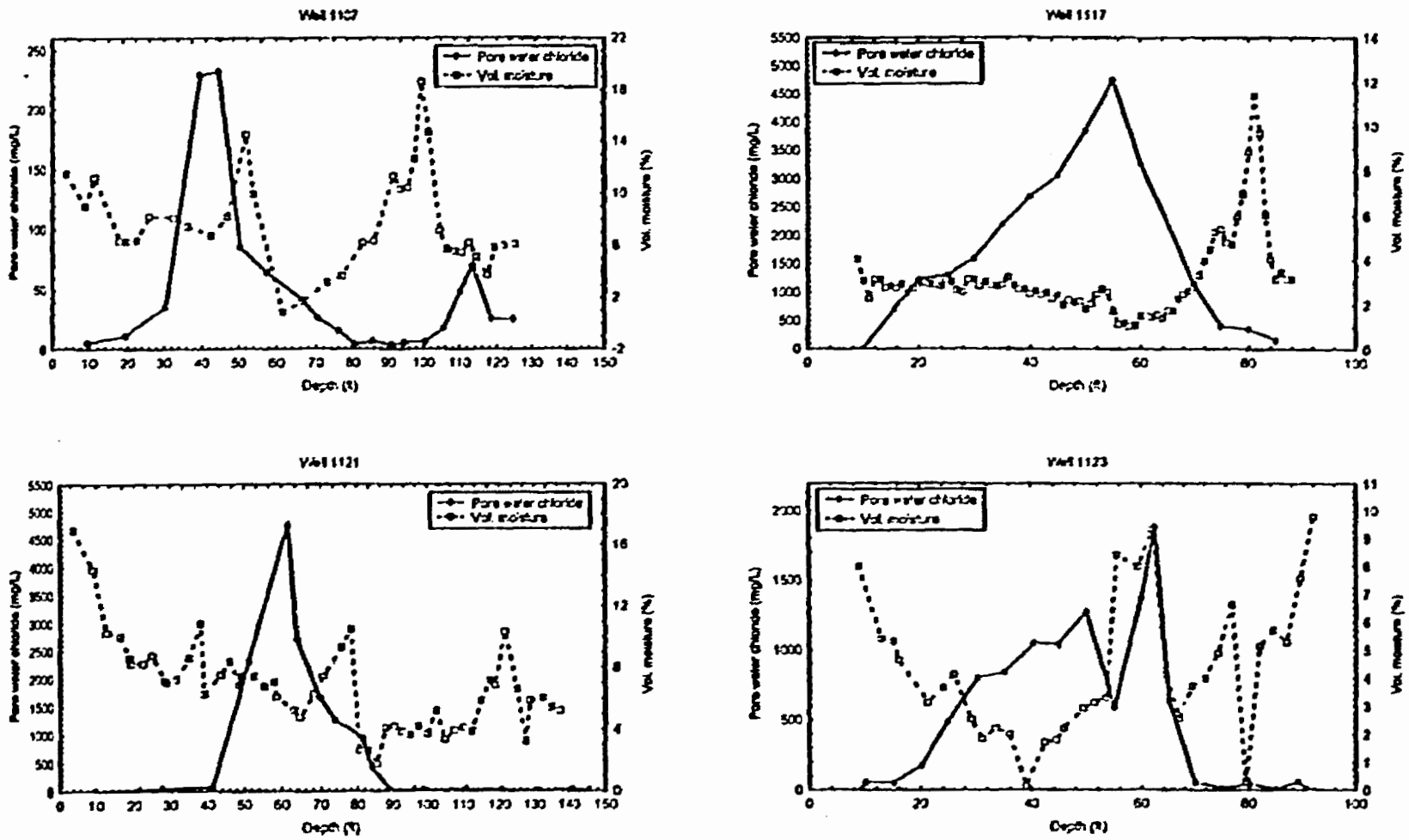

Figure 2. Comparison of pore water chloride and volumetric moisture profiles.

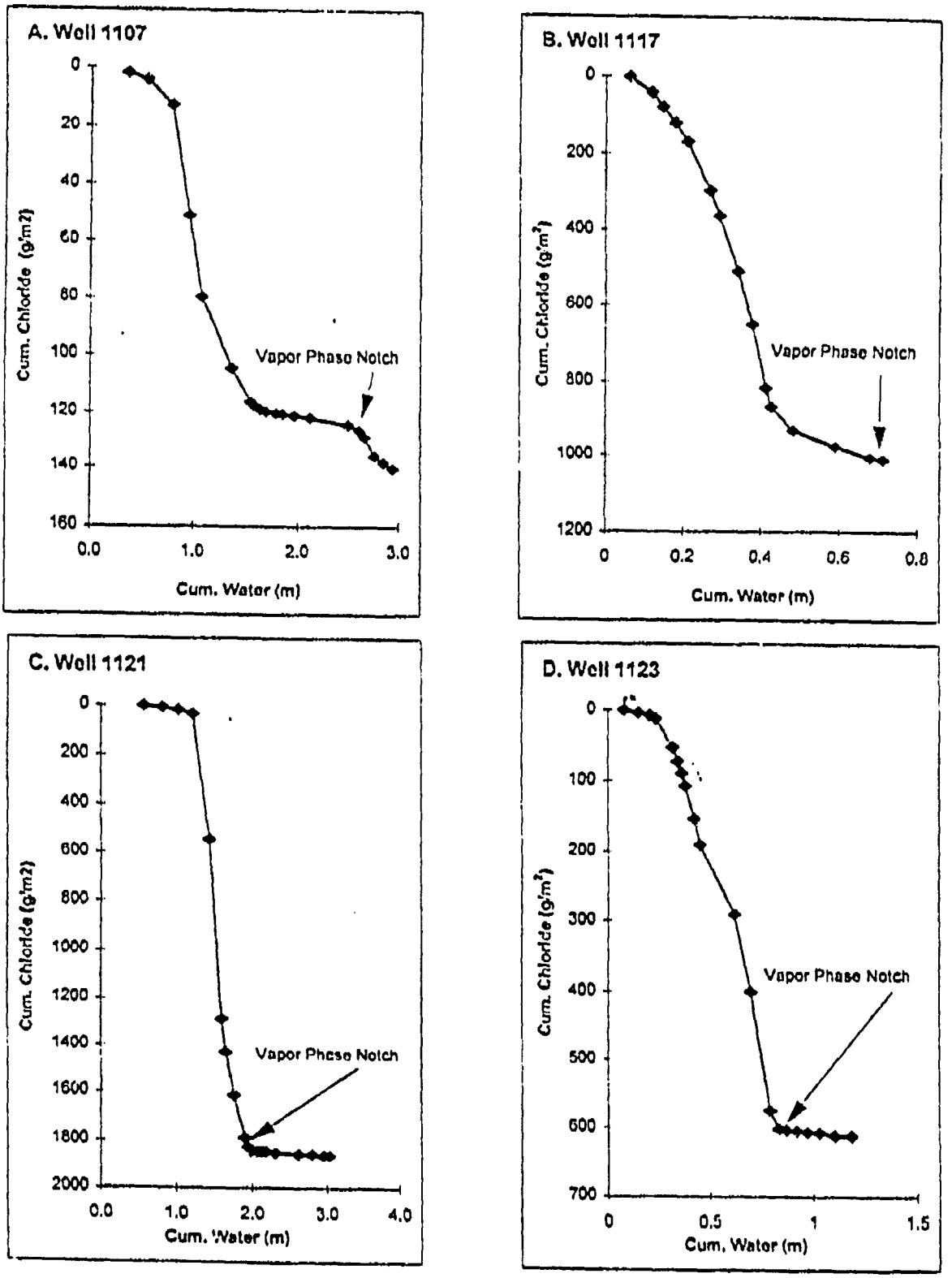

Figure 3. Cumulative water vs. cumulative chloride for wells 1101, 1117, 1121, and 1123.

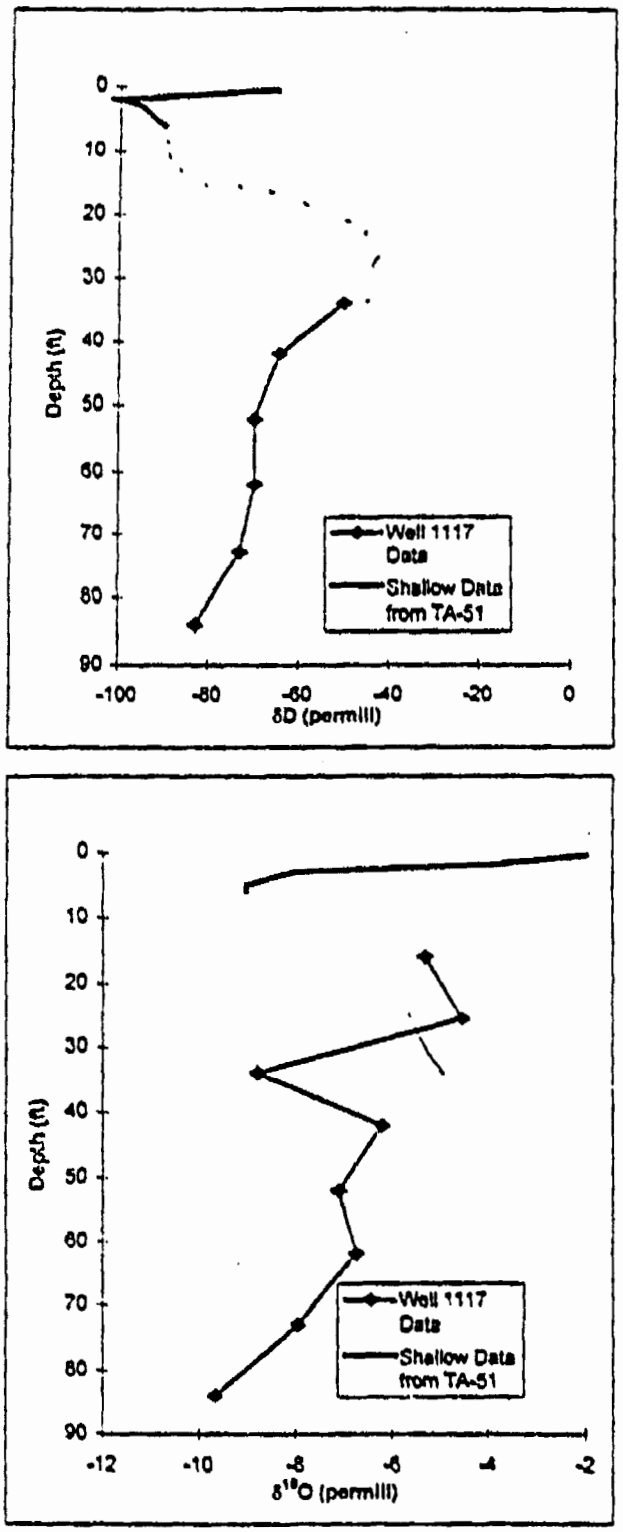

Figure 4. δD and $\delta^{18}O$ in well 1117 pore waters and TA-51 soils.

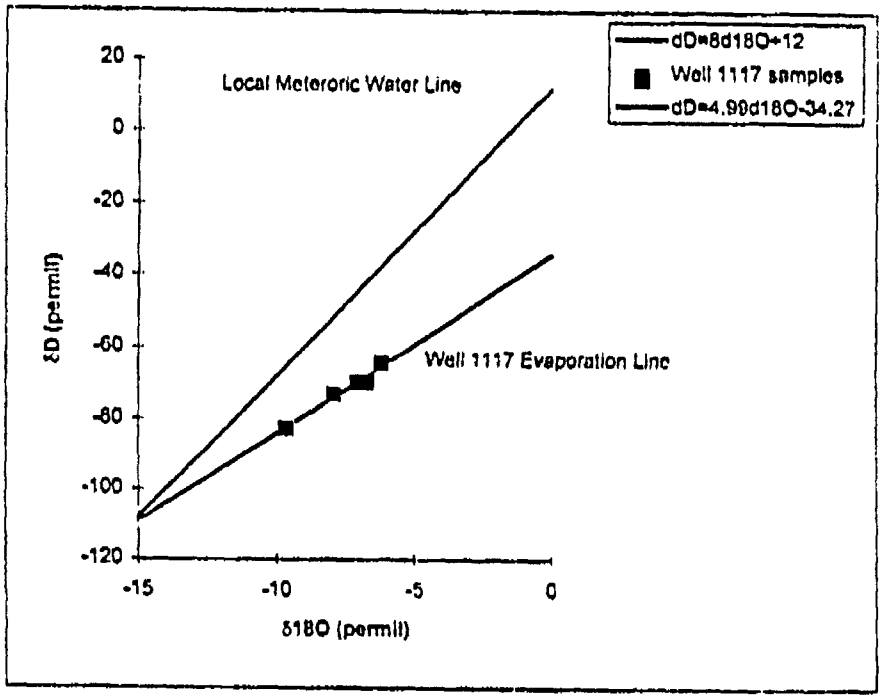

Figure 5. Meteoric water plot of well 1117 waters. The local meteoric water line is from Vuataz and Goff (1986).

Appendix 1a. Data for Area G Core 54-1107

Sampled Depth (ft)	Midpoint (m)	Cl- leachate conc. (mg/L)	DI added (g)	Cl- (mg)	Tuff Dry wt. (g)	θv (%)	ρb (g/cm3)	Pore H2O (L)	Clsw (mg/L)	Clswi (g/m3)	Interval (m)	Interval Clswi (g/m2)	Cum. Clswi (g/m2)	Interval θd (m)	Cum θd (m)
9.7	3.0	0.22	75.17	0.017	46.75	9.01	1.37	0.003	5.4	5.4	4.0	1.9	2	0.4	0.4
19.3	5.8	0.36	75.08	0.027	52.49	6.32	1.37	0.002	11.2	11.2	3.0	2.1	4	0.2	0.6
30.5	9.1	1.35	76.31	0.103	49.51	8.07	1.37	0.003	35.3	35.3	3.0	8.6	13	0.2	0.8
39.5	12.2	7.44	75.29	0.560	49.63	6.75	1.37	0.002	229.1	229.1	2.5	38.7	51	0.2	1.0
44.5	13.4	9.32	75.03	0.699	50.30	8.21	1.37	0.003	232.0	232.0	1.5	28.6	80	0.1	1.1
50.4	15.2	6.07	75.21	0.457	50.48	14.5	1.37	0.005	85.5	85.5	2.0	24.8	105	0.3	1.4
57.4	17.4	3.41	74.91	0.255	55.35	9	1.26	0.004	64.6	64.6	2.0	11.6	116	0.2	1.6
66.3	20.2	0.41	77.45	0.032	58.53	1.7	1.26	0.001	41.6	41.6	1.5	1.1	117	0.0	1.6
70.5	21.3	0.48	75.08	0.036	54.41	3.2	1.26	0.001	26.1	26.1	2.0	1.7	119	0.1	1.6
76	23.2	0.32	75.07	0.024	53.96	3.65	1.26	0.002	15.4	15.4	1.5	0.8	120	0.1	1.7
80.5	24.4	0.14	75.72	0.011	47.58	6.22	1.26	0.002	4.5	4.5	1.5	0.4	120	0.1	1.8
85.5	26.2	0.22	74.99	0.016	50.04	6.31	1.26	0.003	6.6	6.6	1.0	0.4	121	0.1	1.9
90.9	27.7	0.24	75.00	0.018	49.08	11.3	1.2	0.005	3.9	3.9	1.0	0.4	121	0.1	2.0
94.4	28.7	0.30	75.02	0.023	49.01	10.3	1.2	0.004	5.4	5.4	1.5	0.8	122	0.2	2.1
100.4	30.5	0.69	74.99	0.052	51.60	18.6	1.2	0.008	6.5	6.5	2.0	2.4	124	0.4	2.5
105.6	32.3	0.72	75.14	0.054	48.98	7.14	1.14	0.003	17.6	17.6	1.5	1.9	126	0.1	2.6
110	33.5	1.62	75.14	0.122	53.13	5.46	1.14	0.003	47.8	47.8	1.0	2.6	129	0.1	2.7
113.5	34.6	2.01	75.94	0.153	49.05	5.07	1.14	0.002	70.0	70.0	2.0	7.1	136	0.1	2.8
118.5	36.0	0.88	75.10	0.066	50.04	5.86	1.14	0.003	25.7	25.7	1.5	2.3	138	0.1	2.8
124.5	37.8	0.88	76.56	0.067	50.48	6.0534	1.14	0.003	25.1	25.1	1.5	2.3	140	0.1	2.9

..x 1b. Data for Area G Core 54-1117

Sampled Depth (ft)	Midpoint (m)	Cl- leachate conc. (mg/L)	DI Added (g)	Cl- (mg)	Tuff Dry Wt (g)	θv (%)	ρb (g/cm3)	Pore H2O (L)	Clsw (mg/L)	Clswi (g/m3)	Interval	Interval Clswi (g/m2)	Cum. Clswi (g/m2)	Interval θd (m)	Cum θd (m)
9.9	3.0	0.15	74.63	0.01	51.329	3.074	1.37	0.001	10	10	2.0	0.6	1	0.06	0.1
15.5	4.7	9.79	77.32	0.76	52.509	2.838	1.37	0.001	698	698	2.0	39.5	41	0.06	0.1
20	6.1	17.7	75.57	1.34	50.388	2.955	1.37	0.001	1231	1231	1.0	36.4	77	0.03	0.1
25.35	7.7	20.7	74.54	1.54	51.255	3.134	1.37	0.001	1316	1316	1.0	41.2	118	0.03	0.2
30	9.1	27.6	74.33	2.05	55.853	3.149	1.37	0.001	1598	1598	1.0	50.3	169	0.03	0.2
35	10.7	34.2	76.81	2.63	51.627	2.91	1.26	0.001	2203	2203	2.0	128.2	297	0.06	0.3
40	12.2	37.1	74.43	2.76	51.745	2.493	1.26	0.001	2697	2697	1.0	67.2	364	0.02	0.3
45	13.7	49.2	76.38	3.76	63.972	2.418	1.26	0.001	3061	3061	2.0	148.0	512	0.05	0.3
50	15.2	36.6	76.99	2.82	50.114	1.837	1.26	0.001	3856	3856	2.0	141.7	654	0.04	0.4
55	16.8	41.6	77.77	3.24	49.893	1.718	1.26	0.001	4755	4755	2.0	163.4	817	0.03	0.4
60	18.3	26.0	76.89	2.00	51.546	1.495	1.26	0.001	3270	3270	1.0	48.9	866	0.01	0.4
70	21.3	17.5	74.66	1.31	49.020	2.791	1.2	0.001	1146	1146	2.0	64.0	930	0.06	0.5
75.1	22.9	11.4	76.23	0.87	47.428	5.369	1.2	0.002	410	410	2.0	44.0	974	0.11	0.6
80	24.4	17.3	76.96	1.33	50.834	8.87	1.2	0.004	354	354	1.0	31.4	1005	0.09	0.7
85	25.9	3.00	76.48	0.23	53.021	3.149	1.14	0.001	157	157	1.0	4.9	1010	0.03	0.7

Appendix 1c. Data for Area G Core 54-1121

Sampled Depth (ft)	Midpoint (m)	Cl- leachate conc. (mg/L)	DI Added (g)	Cl- (mg)	Tuff Dry Wt (g)	θv (%)	ρb (g/cm3)	Pore H2O (L)	Clsw (mg/L)	Clswl (g/m3)	Interval (m)	Interval Clswl (g/m2)	Cum. Clswl (g/m2)	Interval θd (m)	Cum θd (m)
9.7	3.0	0.15	75.65	0.01	55.92	14.39	1.37	0.006	2	2	4.0	1.1	1	0.6	0.6
21.4	6.4	1.14	74.82	0.09	50.77	8.261	1.37	0.003	28	28	3.0	6.9	8	0.2	0.8
27.9	8.5	1.84	76.24	0.14	53.33	7.157	1.26	0.003	46	46	3.0	9.9	18	0.2	1.0
41.5	12.8	2.80	74.13	0.21	49.73	6.3	1.26	0.002	83	83	3.0	15.8	34	0.2	1.2
51.2	15.5	92.3	74.17	6.85	50.57	7.396	1.26	0.003	2306	2306	3.0	511.8	545	0.2	1.4
61.5	18.9	133	77.36	10.29	52.39	5.216	1.26	0.002	4744	4744	3.0	742.4	1288	0.2	1.6
63.7	19.5	75.7	75.74	5.73	51.21	5.216	1.26	0.002	2705	2705	1.0	141.1	1429	0.1	1.7
69.6	21.3	68.4	74.24	5.08	49.56	7.416	1.2	0.003	1658	1658	1.5	184.4	1613	0.1	1.8
73.7	22.6	63.6	75.87	4.83	49.34	9.324	1.2	0.004	1259	1259	1.5	175.0	1789	0.1	1.9
81.4	24.7	17.0	74.74	1.27	58.12	2.645	1.14	0.001	942	942	1.5	37.4	1827	0.0	1.9
84	25.6	7.37	74.18	0.55	55.76	2.633	1.14	0.001	425	425	1.5	18.8	1844	0.0	2.0
89.2	27.1	0.58	76.50	0.04	54.78	4.058	1.14	0.002	23	23	2.0	1.8	1845	0.1	2.1
96.3	29.3	0.68	74.28	0.05	60.26	3.648	1.14	0.002	25	25	1.5	1.4	1847	0.1	2.1
98.7	30.2	0.53	76.64	0.04	57.58	3.716	1.14	0.002	22	22	1.5	1.2	1848	0.1	2.2
110.9	33.8	0.82	75.43	0.06	49.00	4.081	1.14	0.002	35	35	3.0	4.3	1852	0.1	2.3
120.7	36.9	1.33	75.37	0.10	50.74	10.35	1.12	0.005	21	21	3.0	6.6	1859	0.3	2.6
131.2	39.9	0.17	75.24	0.01	49.32	6.037	1.12	0.003	5	5	3.0	0.9	1860	0.2	2.8
141	43.0	0.96	74.20	0.07	56.29	5.197	1.12	0.003	27	27	3.0	4.3	1864	0.2	2.9
145.7	44.5	0.26	74.79	0.02	48.78	5.197	1.2	0.002	9	9	1.5	0.7	1865	0.1	3.0

Appendix 1d. Data for Area G Core 54-1123.

Sampled Depth (ft)	Midpoint (m)	Cl- leachate conc. (mg/L)	DI Added (g)	Cl- (mg)	Tuff Dry Wt (g)	θv (%)	ρb (g/cm3)	Pore H2O (L)	Clsw (mg/L)	Clswi (g/m3)	Interval (m)	Interval Clswi (g/m2)	Cum. Clswi (g/m2)	Interval θd (m)	Cum θd (m)
9.2	2.80	0.135	75.68	0.010	47.6408	7.97	1.37	0.003	4	4	1.0	0.29	0.29	0.1	0.1
10.2	3.11	1.92	75.84	0.146	53.5126	7.00	1.37	0.003	53	53	1.0	3.7	4	0.1	0.1
15.2	4.63	1.47	76.22	0.112	55.4354	5.32	1.37	0.002	52	52	1.0	2.8	7	0.1	0.2
20.3	6.19	2.79	75.28	0.210	52.3217	3.12	1.37	0.001	176	176	1.0	5.5	12	0.0	0.2
25	7.62	10.4	76.97	0.800	54.6605	4.11	1.37	0.002	488	488	2.0	40.1	52	0.1	0.3
30.5	9.30	12.5	74.37	0.930	58.1434	2.52	1.26	0.001	799	799	1.0	20.1	73	0.0	0.3
35.1	10.70	10.0	75.22	0.752	58.9700	1.98	1.26	0.001	841	841	1.0	16.6	89	0.0	0.4
40.5	12.34	10.1	75.33	0.761	53.9021	1.70	1.26	0.001	1046	1046	1.0	17.8	107	0.0	0.4
45	13.72	13.0	77.95	1.013	55.1873	2.22	1.26	0.001	1043	1043	2.0	46.3	153	0.0	0.4
50	15.24	17.5	78.33	1.371	46.4465	2.92	1.26	0.001	1272	1272	1.0	37.2	190	0.0	0.5
55	16.76	29.6	76.09	2.252	54.1038	8.40	1.2	0.004	595	595	2.0	99.9	290	0.2	0.6
60	18.29	62.5	75.72	4.733	51.9046	7.98	1.2	0.003	1371	1371	1.0	109.4	400	0.1	0.7
62.5	19.05	115	77.23	8.881	60.8377	9.31	1.2	0.005	1881	1881	1.0	175.2	575	0.1	0.8
65	19.81	15.6	74.98	1.170	53.1470	4.12	1.2	0.002	642	642	1.0	26.4	601	0.0	0.8
70	21.34	1.17	75.52	0.088	50.7067	3.71	1.14	0.002	54	54	1.0	2.0	603	0.0	0.9
75	22.86	0.41	75.71	0.031	50.7688	4.89	1.14	0.002	14	14	1.0	0.7	604	0.0	0.9
80	24.38	1.31	74.71	0.098	53.8481	5.15	1.14	0.002	40	40	1.0	2.1	606	0.1	1.0
85	25.91	0.22	74.35	0.016	58.1223	5.70	1.14	0.003	6	6	1.0	0.3	606	0.1	1.0
89	27.13	2.40	77.50	0.186	49.8342	7.57	1.12	0.003	55	55	1.0	4.2	611	0.1	1.1
90.8	27.68	0.26	74.52	0.019	55.7523	8.00	1.12	0.004	5	5	1.0	0.4	611	0.1	1.2